ELSEVIER

Chemical Geology 199 (2003) 233–242

CHEMICAL GEOLOGY
INCLUDING
ISOTOPE GEOSCIENCE

www.elsevier.com/locate/chemgeo

Trace element partitioning between baddeleyite and carbonatite melt at high pressures and high temperatures

Stephan Klemme*, Hans-Peter Meyer

Mineralogisches Institut, Universität Heidelberg, Im Neuenheimer Feld 236, 69120 Heidelberg, Germany

Received 1 December 2000; accepted 19 February 2003

Abstract

Baddeleyite (ZrO_2) is an accessory phase in a wide range of rocks ranging from kimberlites to carbonatites. Despite an increasing interest in baddeleyite especially in the fields of geochronology and petrology, there is, however, no experimental information as to how trace elements partition between baddeleyite and silicate or carbonate melts. To address this problem, hitherto unknown partition coefficients between baddeleyite and carbonatite melt were determined experimentally at high pressures and high temperatures. Experimental run products were analysed for trace elements with secondary ion mass spectrometry and with the electron microprobe. Calculated partition coefficients indicate that U, Th, Hf, Nb and Ta as well as the heavy rare earth elements (HREE) prefer to enter baddeleyite rather than carbonate melts ($D>1$), whereas the light rare earth elements (LREE) and other trace elements behave incompatibly ($D<1$), i.e., they prefer to enter the carbonate melt rather than the baddeleyite crystal. The partition coefficients indicate that baddeleyite may be able to slightly fractionate Zr from Hf during fractional crystallisation of a carbonatite magma ($D^{Zr}/D^{Hf}=1.4$). Moreover, baddeleyite could fractionate U from Th during fractional crystallisation, in a similar manner to garnet.

Keywords: Baddeleyite; ZrO_2; Trace element partitioning; Partition coefficient; Carbonatite

1. Introduction

The mineral baddeleyite (ZrO_2), named after the tea farmer Joseph Baddeley (Fletcher, 1893), has recently become a mineral of interest in geochronology and petrology (e.g., Heaman and LeCheminant, 1993; Schärer et al., 1997; Wingate and Compston, 2000; Amelin and Zaitsev, 2002). Besides the rare occurrences of Baddeleyite in lunar and meteoritic samples, baddeleyite is known to occur as an accessory phase in many different terrestrial rocks such as kimberlites (Schärer et al., 1997; Kerschhofer et al., 2000), alkaline syenites, layered mafic intrusions, gabbro sills and also in carbonatites (e.g., Heaman and LeCheminant, 1993; Reischmann et al., 1995). More than 200 minerals are known from carbonatite rocks, the most important zirconium-bearing phase of which is baddeleyite (ZrO_2) and not zircon as in silicate rocks because of generally lower silica activity in carbonatite melts. Baddeleyite is known to accumulate the high field strength elements (HFSE) and some rare earth elements (REE) (e.g., Reischmann et al., 1995). Despite the increasing attention from both geochronologists (Krogh

* Corresponding author. Fax: +49-6221-544805.
E-mail address: sklemme@min.uni-heidelberg.de (S. Klemme).

0009-2541/03/$ - see front matter © 2003 Elsevier Science B.V. All rights reserved.
doi:10.1016/S0009-2541(03)00081-0

et al., 1987; Wingate and Compston, 2000; Wingate, 2001; Heaman et al., 2002; Santos et al., 2002) and geochemists (e.g., Reischmann et al., 1995), there is no experimental information as to how trace elements (including U, Pb and Th) behave during crystallisation of baddeleyite from silicate or carbonate liquids. This study aims to partially fill this gap by investigating the trace element partitioning between baddeleyites and carbonatite melts at high pressure and high temperature. This information is, of course, necessary for interpreting trace element patterns in carbonatitic baddeleyites or evaluating the effect of baddeleyite fractionation on the trace element budget of a carbonatite melt.

1.1. Carbonatites in crust and mantle

Carbonatites are rare igneous rocks of mantle origin but whether they are primary mantle melts or differentiates is still a matter of contention (Bell and Blenkinsop, 1989; Ionov et al., 1996; Harmer and Gittins, 1998; Dalton and Presnall, 1998; Harmer et al., 1998). In support of the former is the increasing body of experimental and geochemical evidence, which shows that the carbonatitic magmas can be equilibrated with upper mantle lithologies (Wallace and Green, 1988; Yaxley et al., 1991; Dalton and Wood, 1993; Klemme et al., 1995; Yaxley and Green, 1996).

Carbonatite melts are also believed to exert an important role in metasomatic processes in the Earth's upper mantle. Their low viscosity (e.g., Hunter and McKenzie, 1989; Minarik and Watson, 1995) and presumed high contents of trace elements make them effective metasomatic agents. In some cases, major and trace element signatures of peridotite xenoliths (Yaxley et al., 1991, 1998; Dautria et al., 1992; Rudnick et al., 1993; Ionov et al., 1993; Coltorti et al., 1999; Mattielli et al., 1999; Gregoire et al., 2000) and of mantle derived melts (e.g., Hauri et al., 1993) seem to demonstrate the case for metasomatic carbonatite melts in the Earth's mantle. Baddeleyite may also form as an accessory phase during metasomatic infiltration of carbonate melts into peridotite, similar to zircons formed in veins in peridotite xenoliths (Rudnick et al., 1999; Devey et al., 2000).

Partitioning data for accessory phases such as baddeleyite will further our understanding of the trace element budget of naturally occurring carbonatites (e.g., Hamilton et al., 1989) and of metasomatic processes in the crust and the upper mantle which may be caused by carbonate melts (Green and Wallace, 1988; Yaxley et al., 1991, 1998; Klemme et al., 1995; Coltorti et al., 1999; Mattielli et al., 1999).

2. Experiments

2.1. Starting materials

The starting material consisted of mechanical mixes of synthetic $CaCO_3$ and ZrO_2, doped with a range of minor and trace elements (Table 1). The approach chosen here is to equilibrate baddeleyite crystals with carbonatite melts in a simplified chemical system at high pressure and high temperature. As experimental reaction rates in Zr-bearing systems are known to be rather sluggish at low temperatures, with small crystal sizes (Watson and Harrison, 1983; Harrison and Watson, 1983), the present experiments were conducted at relatively high temperatures to promote the attainment of equilibrium in the experiment and crystal growth of baddeleyite from the melt. As the zirconium saturation in carbonatite melts is only poorly understood (Meen et al., 1989), the present experiments were conducted with an arbitrarily chosen value of 5 wt.% ZrO_2 in the starting material. The experiments are part of a wider study investigating the Zr-solubility in silicate and carbonate melts; consequently SiO_2 was also added to the starting mixtures. The experiments, however, are well below zircon stability. No zircon was found in optical and scanning electron microscope (SEM) examination of the experiments; mass balance calculations also indicate no other accessory phase present. Trace elements were added as oxides to the starting material and were subsequently ground under ethanol in an agate mortar for at least 1 h and were stored in an oven at 110 °C. This procedure complicates matters slightly as the starting materials could not be vitrified, as it is usually done in silicate systems (e.g., Klemme et al., 2002), so that complete homogenisation of the starting material cannot be guaranteed. Despite these problems, mass balance calculations involving the starting material, baddeleyite and melt analyses of the run products indicate relatively good agreement. Moreover, the aforementioned matters will not affect the partitioning of trace elements between baddeleyite

Table 1
Experimental run conditions, starting material composition, trace element composition of carbonatite melts and baddeleyites, and calculated partition coefficients

Experimental run conditions												
P (GPa)	1.0	*T* (°C)	1360 °C	Duration (h)	43							
Starting material (ppm)												
	Li	Be	B	Ti	Rb	Sr	Y	Nb	Cs	Ba	La	Ce
	1000	500	1000	650	400	7000	6000	1500	5500	2500	1500	5000
	Pr	Sm	Gd	Lu	Hf	Ta	Pb	Th	U			
	3000	3500	5000	2000	2000	2500	1000	2500	2500			
Experimental run products												
SIMS	Li[a]	Be[a]	B	Si	P[a]	K[a]	Ti	Rb[a]	Sr	Y	Nb	Cs[a]
Baddeleyite	17 (11)	6 (7)	39 (28)	649 (422)	0.5 (4)	23 (21)	918 (117)	4 (3)	120 (76)	22,955 (3479)	2708 (393)	98 (63)
Melt	2159 (213)	913 (43)	2526 (121)	39,012 (2151)	13.0 (14)	252 (55)	1357 (43)	450 (139)	10,553 (184)	6214 (236)	1948 (95)	9092 (1769)
D	0.009 (3)	0.008 (2)	0.018 (5)	0.019 (6)	0.05 (1)	0.11 (3)	0.8 (2)	0.011 (3)	0.013 (4)	4.3 (13)	1.6 (5)	0.013 (4)
	Ba[a]	La	Ce	Pr	Sm	Gd	Lu	Ta	Pb	Th	U	
Baddeleyite	51 (55)	173 (16)	1778 (242)	1565 (219)	6496 (998)	14,580 (2384)	12,272 (2205)	11,562 (2018)	235 (23)	11,038 (2160)	38,168 (7322)	
Melt	6103 (312)	2303 (107)	6149 (257)	3666 (162)	5047 (211)	7928 (366)	1850 (111)	1747 (71)	227 (25)	1806 (92)	1211 (58)	
D	0.010 (3)	0.09 (3)	0.39 (10)	0.59 (1)	1.5 (5)	2.1 (6)	7.7 (23)	7.7 (23)	1.2 (4)	7 (2)	37 (11)	
EMPA	Ti	Y	Nb	Zr	Ce	Pr	Sm	Gd	Lu	Hf	Ta	Th
Baddeleyite	1392 (418)	33,032 (9910)	2993 (898)	350,356 (105,107)	2183 (655)	1843 (553)	8097 (2429)	24,311 (7293)	20,325 (6098)	92,927 (27,878)	31,444 (9433)	23,670 (7101)
Melt	991 (297)	5170 (1551)	1634 (490)	1772 (532)	6176 (1853)	3503 (1051)	3262 (979)	6159 (1848)	1613 (484)	664 (199)	3567 (1070)	2783 (835)
D	1.4 (4)	6.4 (19)	1.8 (5)	198 (59)	0.4 (1)	0.5 (2)	2.5 (7)	3.9 (12)	13 (4)	140 (42)	9 (3)	9 (3)

Experimental run conditions, nominal trace element composition of starting material and compositions of baddeleyites equilibrated with carbonatite melts (ppm). *P* = pressure, *T* = temperature, h = hours. The experimental run products were analysed both with SIMS and with the EMPA. Also shown are calculated partition coefficients (*D*). Note that mass balancing starting material, mineral and melt analyses gives reasonable results for most trace elements, given the fact that trace elements had to be added as oxides and could only be homogenized by manual mixing (see text for details). Numbers in parentheses indicate the standard deviation of the mean of several analyses, e.g., 5.1 (3) should be read as 5.1 ± 0.3 and 0.574 (15) should be read as 0.574 ± 0.015. Note that, because of very low ion yield of Pb for the quenched melts, the Pb-partition coefficient should only be used with caution. The uncertainties of calculated partition coefficients were estimated at 30%, although the reproducibility of the individual analyses is much better for most elements. At least five measruements were done for both crystals and melts. See text for further information and discussion.

[a] Note that baddeleyite analyses for some elements (Li, B, Ba, K, Rb, Cs, P) show substantially larger scatter than 30% relative, so that calculated partition coefficients should only be used with caution.

and melts as high run temperatures and extremely mobile melts ensure rapid equilibration during the runs even though the starting material may not have been completely homogenized.

2.2. Experimental and analytical techniques

High-pressure high-temperature experiments were carried out in a 1.27-cm end-loaded piston-cylinder apparatus at Bristol University. The pressure assembly consists of two inner parts of alumina surrounded by concentric shells of a graphite heater, a soft glass tube of pyrex and an outermost sleeve of NaCl, pressed to >95% of the theoretical density. This low-friction assembly requires only minimal friction correction of −3% (Klemme and Dalpe, 2003, Brodholt and Wood, 1994). Runs were performed using the "piston-in" routine. First, a pressure of ~0.25 GPa was applied before heating the sample to 450 °C to soften the glass. During compression to the final run pressure, temperatures were raised simultaneously. Pressure was kept constant during runs to within ±0.02 GPa by manual adjustment if necessary. Starting materials were welded into platinum capsules, which were placed in holes in the lower alumina inner part and separated from the thermocouple by a 0.5-mm Al_2O_3 disc. Temperatures were measured with calibrated $W_{95}Re_5$–$W_{75}Re_{25}$ thermocouples inserted axially into the assembly using four-bore high-purity Al_2O_3 tubing. It was found necessary to use soft stainless steel top plugs to close the upper part of the assembly during the run to prevent oxidation of the thermocouple. No correction was made for the dependence of thermocouple emf on pressure. The sample was placed in the hotspot of the assembly. Temperature uncertainties are estimated to be less than 15 °C. All experiments were conducted at a pressure of 1.0 GPa. The experiments were hold at a temperature of 1400 °C for 25 min and then slowly cooled (5°/min) to 1360 °C (to promote grain growth), where the experiments were held for 43 h.

The experimental run products were sectioned longitudinally with a low-speed wafering saw and one-half was mounted in epoxy resin and carefully polished to 0.25 μm using diamond pastes. Run products were carbon-coated for electron microprobe analysis (EMPA) and gold-coated for ion probe analysis.

Trace elements were determined by secondary ion mass spectrometry (SIMS) on a Cameca ims 4f ion microprobe at the University of Edinburgh, using a 10.69-kV primary beam of oxygen ions. Positive secondary ions were accelerated to 4.5 keV, with an offset of 75 eV to reduce the transmission of molecular ion species. The energy window was set at 25 eV and primary beam currents were set to 2 nA, resulting in a spatial resolution of the beam of ca. 10–15 μm diameter. The following masses were counted: ^{7}Li, ^{9}Be, ^{11}B, ^{30}Si, ^{31}P, ^{39}K, ^{42}Ca, ^{47}Ti, ^{85}Rb, ^{88}Sr, ^{89}Y, ^{93}Nb, ^{96}Zr, ^{133}Cs, ^{138}Ba, ^{139}La, ^{140}Ce, ^{141}Pr, ^{149}Sm, ^{160}Gd, ^{175}Lu, ^{178}Hf, ^{181}Ta, ^{208}Pb, ^{232}Th, ^{238}U and ratioed to Ca, after calibration on NIST standard SRM 610. The Ca content of baddeleyites and quenched melts were independently measured with the electron microprobe. Mass 130.5 was used to monitor the background; all analyses reported here have zero background counts. Possible ZrH interference on ^{93}Nb was not monitored; quoted Nb partition coefficients have to be considered as maximum values.

To cross check the ion probe analyses, a number of selected minor and trace elements were determined by wavelength dispersive electron microprobe analysis on a four spectrometer CAMECA SX 51 electron microprobe at Heidelberg University, using 15 kV accelerating voltage and 20 nA probe current for baddeleyite, and 5 nA, with a broader beam, for carbonates. Due to the fact that a large number of elements were analysed, much care was taken to identify first and higher order interferences with qualitative scans at low spectometer speed. We took great care to place the correct background positions to avoid possible interferences. Quantitative analyses were performed after calibration on well-characterized oxide, metal and rare earth phosphates (Jarosewich and Boatner, 1991).

Contamination of crystal analyses by surrounding matrix material can be a significant problem when crystal size is only slightly larger than the diameter of the beam (cf. Blundy and Dalton, 2000) Contamination is most apparent for the most incompatible elements, such as Ba or Cs. In this study, Ba and Cs were used as a monitor, which indicates that contamination was not a significant factor. There is presently no rigorous information about the ion yield for a carbonate matrix during SIMS analysis, but the relative agreement of calculated partition coefficients between electron microprobe (EMP) and ion microp-

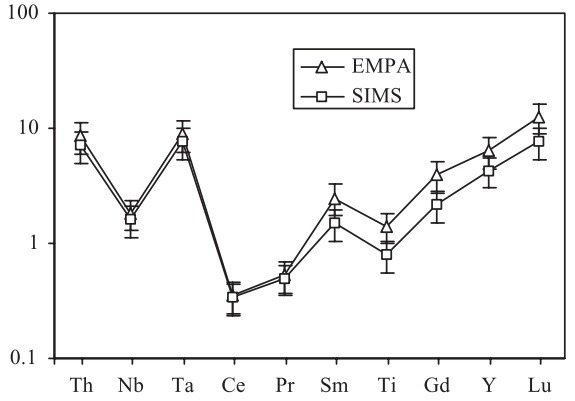

Fig. 1. A comparison of partition coefficients calculated from ion probe analyses (SIMS) and EMPA, respectively. Note that, because of detection limits, only some selected elements could be analysed with the electron microprobe. There is reasonable agreement between the two analytical techniques.

robe analyses (see below, Figs. 1 and 2) indicates no significant problems. Blundy and Dalton (2000) found no significant influence of ion-yield differences between silicate and carbonate matrixes on calculated partition coefficients. Furthermore, their clinopyroxene/ carbonatite melt partition coefficients (using ion microprobe techniques) are in virtually perfect agreement with results by Klemme et al. (1995) who used Laser Ablation ICPMS techniques. Note, however, that, although there is rather good agreement of partition coefficients between baddeleyite and melt derived from SIMS and EMP analyses, respectively, there is much larger scatter in the actual concentrations of baddeleyite and melts. This scatter may be caused by matrix effects that could not be accounted for because of a lack of suitable standard materials.

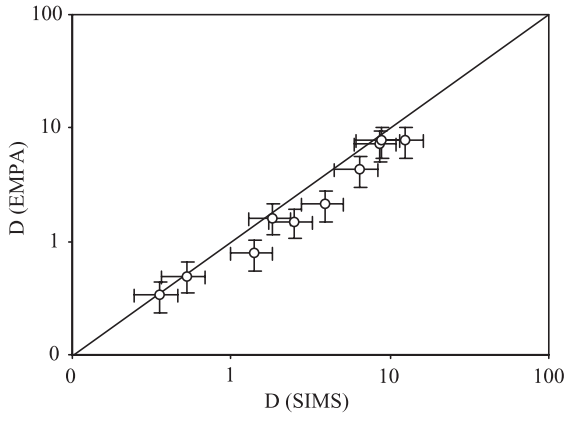

Fig. 2. A comparison of partition coefficients calculated from ion probe analyses (SIMS) and EMPA, respectively. Within the uncertainties, reasonable agreement is found between the results derived with different analytical methods.

3. Results and discussion

The experimental run products contained baddeleyite crystals and a quenched carbonate melt. The baddeleyite crystals were generally 10–40 μm across and showed no signs of zonation or inclusions (Fig. 3). The quenched carbonatite melt consisted of a very fine intergrowth of carbonate and submicron, unidentifiable oxide crystals. As the present experiments were performed at high temperatures (i.e., in the stability field of tetragonal ZrO_2)

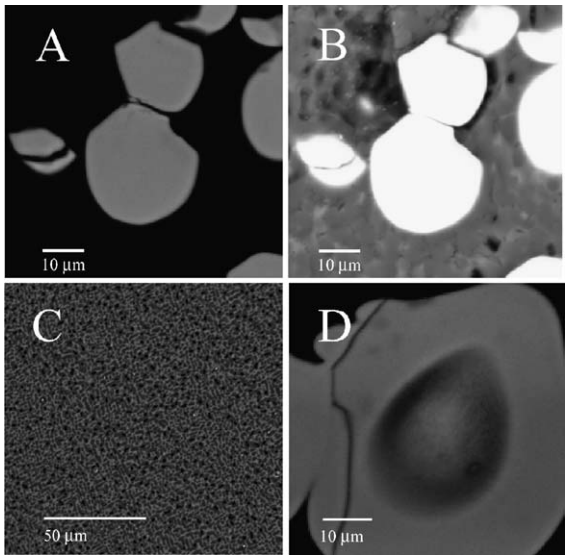

Fig. 3. Back-scattered electron (BSE) images of the experimental run products taken with a SEM: (A) Baddeleyite crystals surrounded by quenched carbonatite melt. Most baddeleyite crystals develop only some crystal faces and appear rounded. Note that there is a strong imaging contrast between baddeleyite and quenched carbonate melt. (B) Same as A, only this picture was taken with different SEM settings. (C) Large areas of quenched carbonatite melt in top of the capsule. See text for details and discussion. (D) Ion probe ablation pits within a large baddeleyite crystal.

baddeleyites showed no sign of twinning, a phenomenon frequently observed in naturally occurring samples (Bischoff and Rühle, 1983; Wingate and Compston, 2000). As McCullough and Trueblood (1959) pointed out, most natural baddeleyites are twinned due to minimisation of crystal shape change during transition from tetragonal to monoclinic ZrO_2, which occurs around 1150 °C at atmospheric pressure (Smith and Newkirk, 1965; Butterman and Foster, 1967). The effect of pressure and bulk composition on this transition is unknown. This means that most carbonatites must have fractionated baddeyite at much higher temperatures than commonly assumed. As most natural baddeleyites, therefore, appear to have *crystallised* from the magma in tetragonal symmetry, the present study only investigates the trace element partitioning between tetragonal baddeleyite and carbonate melts.

3.1. Trace element partitioning

Trace element concentrations in run products and calculated partition coefficients for baddeleyite/melt pairs are listed in Table 1. The partition coefficients are depicted in Fig. 4. The heavier rare earth elements (HREE), most high field strength elements (Zr, Hf, Nb, Ta) and U and Th are compatible in baddeleyite (i.e., $D>1$), whereas the light elements (Li, B, Be), the large ion lithophile elements (K, Cs, Rb, Ba) and the light rare earth elements (LREE) are incompatible.

There are a number of possible substitution mechanisms capable of maintaining charge balance in baddeleyites when high concentrations of 2+, 3+ and 5+ ions are incorporated into the baddeleyite structure. For example, a combined exchange of Ca^{2+} and trivalent ions such as the rare earth elements could charge balance most 5+ ions such as Nb and Ta (Lumpkin, 1999). Moreover, oxygen vacancies may also be of importance in baddeleyites (Platzer et al., 1997). Note that synthetic zirconia-based ceramics incorporate high concentrations of trivalent ions such as Y^{3+} to stabilize cubic and tetragonal zirconia ceramics to lower temperatures. In a systematic study of oxygen vacancies as a function of composition, Platzer et al. (1997) found a systematic increase of oxygen vacancies with increasing content of trivalent ions in zirconia, which indicates that oxygen vacancies play a major role in the substitution of trivalent ions into the ZrO_2 structure. The same mechanism is expected to occur in baddeleyites, but probably to a somewhat lesser extent.

3.2. Interpretation of the results

The present data are, to our knowledge, the only available partition coefficients between baddeleyite

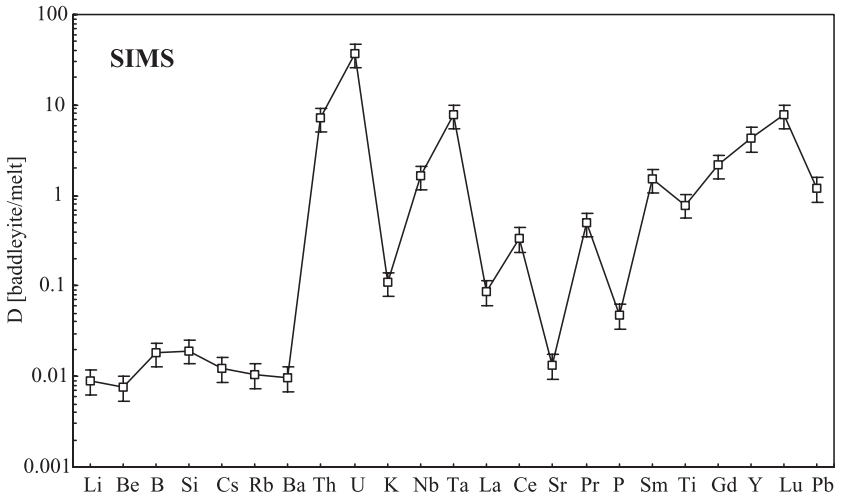

Fig. 4. Partition coefficients between baddeleyite and carbonatite melts (D baddeleyite/melt) as measured with secondary ion mass spectrometry.

and carbonate melts. To interpret the new partitioning data for baddeleyite and carbonatite melt, the crystal melt partitioning model of Wood and Blundy (1997) was employed which is based on the well known observation that mineral melt partition coefficients follow a parabolic trend when plotted against the cation radius of the elements of interest (e.g., Onuma et al., 1968). Quantification of the observed trends were attempted by Beattie (1994) and Blundy and Wood (1994) who employed lattice strain models, theoretically founded by Brice (1975) among others. In the model of Blundy and Wood (1994), trace element partitioning on a given structural site is characterised by the size radius (r_0), its Young's modulus (E) and the strain free partition coefficient D_0 for an element with an ideal radius r_0:

$$D_i = D_0 \exp\left(\frac{-4\pi E N_A\left(\frac{r_0}{2}(r_i - r_0)^2 + \frac{1}{3}(r_i - r_0)^3\right)}{RT}\right) \quad (1)$$

N_A is Avogadro's number, R is the universal gas constant and T is temperature in Kelvin. Least square fitting routines were employed to derive best-fit values for r_0, D_0 and E for the experimentally determined partitioning of the trivalent ions (rare earth elements and others) and for the 4+ ions. Standard deviations of multiple analyses (cf. Table 1) were used to weight the fits. A number of assumptions and constraints were applied: All trace and minor elements partition exclusively into one site in tetragonal baddeleyite in octahedral coordination. Plots of ionic radius versus experimentally determined partition coefficients (Fig. 5) indicate a very good agreement between theory and experiment. For the 3+ ions, the data indicate an unstrained site radius $r_0 = 0.814 \pm 0.06$, a strain free partition coefficient $D_0 = 8.7 \pm 5.6$ and a Young's modulus $E = 328 \pm 146$ GPa. For 4+ ions on the same site, fits indicate $r_0 = 0.791 \pm 0.003$ (in good agreement with the 3+ ions), $D_0 = 464 \pm 123$ and $E = 913 \pm 72$ GPa. The effective Young's modulus for baddeleyite increases with increasing charge, as previously observed for pyroxenes (Wood and Blundy, 1997; Hill et al., 2000), whereas the unstrained site radius (r_0) remains virtually identical (within the uncertainties) indicating that all trace

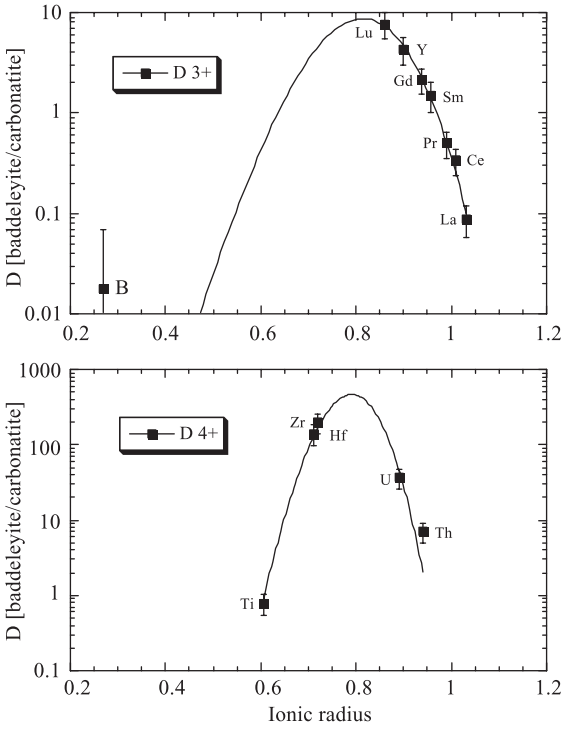

Fig. 5. Partition coefficients between baddeleyite and carbonatite melts shown in order of increasing ion radius. Depicted are 3+ and 4+ ions, respectively. Curves drawn through a series of homovalent cations are obtained by using a weighted least squares fit to Eq. (1). See text for further discussion. Ionic radii are from Shannon (1976) and are given in Å.

elements enter the same site. Although the oxygen fugacity of the experiments was unbuffered, the well-behaved fit of U on the 4+ ions curve (Fig. 5) seems to indicate that most U is present in the 4+ valence state. Furthermore, Ce fits well on the parabolic curve as defined by the trivalent ions (Fig. 5), which may be taken as further evidence for rather reducing conditions during the experiments.

At present, there are no trace element partition coefficients between baddeleyite and undersaturated silicate melts with which we could compare our data. However, based on previous experiments for clinopyroxene trace element partitioning in carbonatite and silicate systems (Klemme et al., 1995; Blundy and Dalton, 2000), no large differences between D^{badd}(carbonatite) and D^{badd}(silicate) are expected. Nevertheless, experimental data are needed to confirm this.

3.3. Implications for the trace element budget of carbonatites and for metasomatic processes in the upper mantle

Zr and Hf are very difficult to separate from each other, due to very similar size of the 4+ cations. The new partition coefficients (Fig. 4), however, indicate that baddeleyite may be able to slightly fractionate Zr from Hf during fractional crystallisation of a carbonatite magma ($D^{Zr}/D^{Hf} = 1.4$), the extent of the resulting Zr/Hf fractionation depends, of course, on the amount of baddeleyite that crystallised from the magma and the degree of partial melting. This could be another possible explanation for the Zr/Hf fractionation observed in some naturally occurring carbonatites that are generally accepted to be low degree partial melts. Hamilton et al. (1989) proposed that Zr and Hf could be fractionated between immiscible carbonate and silicate melts, a result that has recently been questioned by Veksler et al. (1998). Although there is clearly a lack of reliable Zr and Hf trace element data in the literature (not only for carbonatites), it should be mentioned that not all carbonatites exhibit Zr/Hf fractionation (Nelson et al., 1988), perhaps due to the lack of or only small amount of baddeleyite fractionation during crystallisation of the carbonatite magma. Furthermore, baddeleyites and zircons with unusually high Zr/Hf ratios (Zr/Hf = 52–81; Heaman et al., 1990; Schärer et al., 1997) have been reported in the literature. If precipitated from low degree carbonatitic melts, baddeleyite fractionation could cause these high Zr/Hf ratios. High Zr/Hf ratios in whole rock nephelinites, carbonatites and metasomatized mantle rocks (Dupuy et al., 1992; Rudnick et al., 1993; Ionov et al., 1994) could have been caused by similar processes.

The present results show that both Th and U are compatible in baddeleyite. Moreover, baddeleyite fractionates U from Th during fractional crystallisation, in a similar manner to garnet. It has recently been demonstrated that Zr-bearing phases can be precipitated from metasomatic fluids or melts in subduction zone environments (Della Ventura et al., 2000; de Hoog and van Bergen, 2000; Hornig and Wörner, 1991). The possible role of accessory minerals like baddeleyite in subduction zones or mantle metasomatic processes, however, remains highly speculative until further evidence emerges and is beyond the scope of this paper.

Acknowledgements

The experiments were done at Bristol University. Thanks to Drs. J.A. Dalton, J.D. Blundy, B.J. Wood and other members of the CETSEI group at Bristol for discussions. SK acknowledges generous funding from the European Union as a Marie-Curie Individual Fellow. Many thanks also to Richard Hinton and John Craven for help and support at the NERC ion probe facility in Edinburgh. Also thanks to Drs. J. Hermann and E. Hauri whose critical reviews helped to substantially improve the manuscript. **[RR]**

References

Amelin, Y., Zaitsev, A.N., 2002. Precise geochronology of phoscorites and carbonatites: the critical role of U-series disequilibrium in age interpretations. Geochim. Cosmochim. Acta 66, 2399–2419.

Beattie, P., 1994. Systematic and energetics of trace-element partitioning between olivine and silicate melts-implications for the nature of mineral melt partitioning. Chem. Geol. 117, 57–71.

Bell, K., Blenkinsop, J., 1989. Neodymium and strontium isotope geochemistry of carbonatites. In: Bell, K. (Ed.), Carbonatites—Genesis and Evolution. Unwin Hyman, London, pp. 278–300.

Bischoff, E., Rühle, M., 1983. Twin boundaries in monoclinic ZrO_2 particles confined in a mullite matrix. J. Am. Ceram. Soc. 66, 123–127.

Blundy, J.D., Dalton, J.A., 2000. Experimental comparison of trace element partitioning between clinopyroxene and melt in carbonate and silicate systems, and implications for mantle metasomatism. Contrib. Mineral. Petrol. 139, 356–371.

Blundy, J.D., Wood, B.J., 1994. Prediction of crystal-melt partition coefficients from elastic moduli. Nature 372, 452–454.

Brice, J.C., 1975. Some thermodynamic aspects of the growth of strained crystals. J. Cryst. Growth 28, 249–253.

Brodholt, J.P., Wood, B.J., 1994. Measurement of the PVT properties of water to 25 kbars and 1600°C from synthetic fluid inclusions in corundum. Geochim. Cosmochim. Acta 58, 2143–2148.

Butterman, W.C., Foster, W.R., 1967. Zircon stability and the ZrO_2–SiO_2 phase diagram. Am. Mineral. 52, 880–885.

Coltorti, M., Bonadiman, C., Hinton, R.W., Siena, F., Upton, B.G.J., 1999. Carbonatite metasomatism of the oceanic upper mantle: evidence from clinopyroxenes and glasses in ultramafic xenoliths of Grande Comore. Indian Ocean. J. Petrol. 40, 133–165.

Dalton, J.A., Presnall, D.C., 1998. Carbonatitic melts along the solidus of model lherzolite in the system CaO–MgO–Al_2O_3–SiO_2–CO_2 from 3 to 7 GPa. Contrib. Mineral. Petrol. 131, 123–135.

Dalton, J.A., Wood, B.J., 1993. The compositions of primary carbonate melts and their evolution through wallrock reaction in the mantle. Earth Planet. Sci. Lett. 119, 511–525.

Dautria, J.M., Dupuy, C., Takherist, D., Dostal, J., 1992. Carbonatite metasomatism in the lithospheric mantle: peridotitic xenoliths from a melilititic district of the Sahara basin. Contrib. Mineral. Petrol. 111, 37–52.

de Hoog, J.C.M., van Bergen, M.J., 2000. Volatile-induced transport of HFSE, REE, Th and U in arc magmas: evidence from zirconolite-bearing vesicles in potassic lavas of Lewotolo volcano (Indonesia). Contrib. Mineral. Petrol. 139, 485–502.

Della Ventura, G., Bellatreccia, F., Williams, C.T., 2000. Zirconolite, with significant REEZrNb(Mn,Fe)O_7, from a xenolith of the Laacher See eruptive center, Eifel volcanic region, Germany. Can. Mineral. 38, 57–65.

Devey, C.W., Hemond, C., Stoffers, P., 2000. Metasomatic reactions between carbonated plume melts and mantle harzburgite: the evidence from Friday and Domingo Seamounts (Juan Fernandez chain, SE Pacific). Contrib. Mineral. Petrol. 139, 68–84.

Dupuy, C., Liotard, J.M., Dostal, J., 1992. Zr/Hf fractionation in intraplate basaltic rocks: carbonatite metasomatism in the mantle source. Geochim. Cosmochim. Acta 56, 2417–2423.

Fletcher, L., 1893. On baddeleyite (native zirconia), a new mineral from Rakwana, Ceylon. Min. Mag. 10, 148–160.

Green, D.H., Wallace, M.E., 1988. Mantle metasomatism by ephemeral carbonatite melts. Nature 336, 459–462.

Gregoire, M., Moine, B.N., O'Reilly, S.Y., Cottin, J.Y., Giret, A., 2000. Trace element residence and partitioning in mantle xenoliths metasomatized by highly alkaline, silicate-and carbonate-rich melts (Kerguelen Islands, Indian Ocean). J. Petrol. 41, 477–509.

Hamilton, D.L., Bedson, P., Esson, J., 1989. The behaviour of trace elements in the evolution of carbonatites. In: Bell, K. (Ed.), Carbonatites—Genesis and Evolution. Unwin Hyman, London, pp. 405–427.

Harmer, R.E., Gittins, J., 1998. The case for primary, mantle-derived carbonatite magma. J. Petrol. 39, 1895–1903.

Harmer, R.E., Lee, C.A., Eglington, B.M., 1998. A deep mantle source for carbonatite magmatism: evidence from the nephelinites and carbonatites of the Buhere district, SE Zimbabwe. Earth. Planet. Sci. Lett. 158, 131–142.

Harrison, T.M., Watson, E.B., 1983. Kinetics of zircon dissolution and zirconium diffusion in granitic melts of variable water-content. Contrib. Mineral. Petrol. 84, 66–72.

Hauri, E.H., Shimizu, N., Dieu, J.J., Hart, S.R., 1993. Evidence for hotspot-related carbonatite metasomatism in the oceanic upper mantle. Nature 365, 221–227.

Heaman, L.M., LeCheminant, A.N., 1993. Paragenesis and U–Pb systematics of baddeleyite (ZrO_2). Chem. Geol. 110, 95–126.

Heaman, L.M., Bowins, R., Crocket, J., 1990. The chemical composition of igenous zircon suites—implications got geochemical trace studies. Geochim. Cosmochim. Acta 54, 1597–1607.

Heaman, L.M., Srivastava, R.K., Sinha, A.K., 2002. A precise U–Pb zircon/baddeleyite age for the Jasra igneous complex, Karbi-Analong District, Assam, NE India. Current Science 82, 744–748.

Hill, E., Wood, B.J., Blundy, J.D., 2000. The effect of Ca-Tschermaks component of trace element partitioning between clinopyroxene and silicate melt. Lithos 53, 203–215.

Hornig, I., Wörner, G., 1991. Zirconolite-bearing ultra-potassic veins in a mantle xenolith from Mt. Melbourne volcanic field, Victoria Land, Antarctica. Contrib. Mineral. Petrol. 106, 355–366.

Hunter, R.H., McKenzie, D., 1989. The equilibrium geometry of carbonate melt in rocks of mantle composition. Earth. Planet. Sci. Lett. 92, 347–356.

Ionov, D.A., Dupuy, C., O'Reilly, S.Y., Kopylova, G.M., Genshaft, Y.S., 1993. Carbonated peridotitic xenoliths from Spitsbergen: implications for trace element signature of mantle carbonate metasomatism. Earth. Planet. Sci. Lett. 119, 283–297.

Ionov, D.A., Hofmann, A.W., Shimizu, N., 1994. Metasomatism-induced melting in mantle xenoliths from Mongolia. J. Petrol. 35, 753–785.

Ionov, D.A., O'Reilly, S.Y., Genshaft, Y., Koplova, M.G., 1996. Carbonate-bearing mantle peridotite xenoliths from Spitsbergen: phase relationships, mineral compositions and trace element residence. Contrib. Mineral. Petrol. 125, 375–392.

Jarosewich, E., Boatner, L.A., 1991. Rare-earth element reference samples for electron microprobe analysis. Geostand. Newsl. 15, 397–399.

Kerschhofer, L., Schärer, U., Deutsch, A., 2000. Evidence for crystals from the lower mantle: baddeleyite megacrysts of the Mbuji Mayi kimberlite. Earth. Planet. Sci. Lett. 179, 219–225.

Klemme, S., Dalpe, C., 2003. Trace element partitioning between apatite and carbonatite melt. Am. Mineral. 88, 639–646.

Klemme, S., van der Laan, S.R., Foley, S.F., Günther, D., 1995. Experimentally determined trace and minor element partitioning between clinopyroxene and carbonatite melt under upper mantle conditions. Earth. Planet. Sci. Lett. 133, 439–448.

Klemme, S., Blundy, J.D., Wood, B.J., 2002. Experimental constraints on major and trace element partitioning during partial melting of eclogite. Geochim. Cosmochim. Acta 66, 3109–3123.

Krogh, T.E., Corfu, F., Davis, D.W., Dunning, G.R., Heaman, L.M., Kamo, S.L., Machado, N., Greenough, J.D., Nakamura, E., 1987. Precise U–Pb isotopic ages of diabase dykes and mafic to ultramafic rocks using trace amounts of baddeleyite and zircon. In: Halls, H.C., Fahrig, W.F. (Eds.), Mafic Dyke Swarms. Geological Association of Canada Spec. Pap., pp. 147–152.

Lumpkin, G.R., 1999. Physical and chemical characteristics of baddeleyite (monoclinic zirconia) in natural environments: an overview and case study. J. Nucl. Mater. 274, 206–217.

Mattielli, N., et al., 1999. Evolution of heterogeneous lithospheric mantle in a plume environment beneath the Kerguelen Archipelago. J. Petrol. 40, 1721–1744.

McCullough, J.D., Trueblood, K.N., 1959. The crystal structure of baddeleyite (monoclinic ZrO_2). Acta Crystallogr. 12, 507–511.

Meen, J.K., Ayers, J.C., Fregeau, A., 1989. A model of mantle metasomatism by carbonated alkaline melts: trace element and isotopic compositions of mantle source regions of carbonatite and other continental igneous rocks. In: Bell, K. (Ed.), Carbonatites—Genesis and Evolution. Unwin Hyman, London, pp. 464–499.

Minarik, W.G., Watson, E.B., 1995. The interconnectivity of carbonatite melt at low melt fraction. Earth. Planet. Sci. Lett. 133, 423–437.

Nelson, D.R., Chivas, A.R., Chappell, B.W., McCulloch, M.T., 1988. Geochemical and isotopic systematics in carbonatites

and implications for the evolution of ocean-island basalts. Geochim. Cosmochim. Acta 52, 1–17.

Onuma, N., Higuchi, H., Wakita, H., Nagasawa, H., 1968. Trace element partitioning between two pyroxenes and the host lava. Earth. Planet. Sci. Lett. 5, 47–51.

Platzer, R., Karapetrova, E., Zacate, M.O., Gardner, J.A., Sommers, J.A., Evenson, W.E., 1997. Oxygen vacancies in zirconia. Mat. Sci. Forum 239–241, 57–60.

Reischmann, T., Brügmann, G.E., Jochum, K.P., Todt, W.A., 1995. Trace element and isotopic composition of baddeleyite. Mineral. Petrol. 53, 155–164.

Rudnick, R.L., McDonough, W.F., Chappell, B.W., 1993. Carbonatite metasomatism in the northern tanzanian mantle: petrographic and geochemical characteristics. Earth. Planet. Sci. Lett. 114, 463–475.

Rudnick, R.L., Ireland, T.R., Gehrels, G., Irving, A.J., Chesley, J.T., Hanchar, J.M., 1999. Dating mantle metasomatism: U–Pb geochronology of zircons in cratonic mantle xenoliths from Montana and Tanzania. In: Gurney, J.J., Pascoe, M.D., Richardson, S.H. (Eds.), Seventh International Kimberlite Conference, Capetown, pp. 728–735.

Santos, J.O.S., Hartmann, L.A., McNaughton, N.J., Fletcher, I.R., 2002. Timing of mafic magmatism in the Tapajo's Province (Brazil) and implications for the evolution of the Amazon Craton: evidence from baddeleyite and zircon U–Pb SHRIMP geochronology. J. South Am. Earth Sci. 15, 409–429.

Schärer, U., Corfu, F., Demaiffe, D., 1997. U–Pb and Lu–Hf isotopes in baddeleyite and zircon megacrysts from the Mbuji-Mayi kimberlite: constraints on the subcontinental mantle. Chem. Geol. 143, 1–16.

Shannon, R.D., 1976. Revised effective ionic radii and systematic studies of interatomic distances in halides and chalcogenides. Acta Crystallogr. 32, 751–767.

Smith, D.K., Newkirk, H.W., 1965. The crystal structure of baddeleyite (monoclinic ZrO_2) and its relation to polymorphism of ZrO_2. Acta Crystallogr. 18, 983–991.

Veksler, I.V., Petibon, C., Jenner, G.A., Dorfman, A.M., Dingwell, D.B., 1998. Trace element partitioning in immiscible silicate–carbonate liquid systems: an initial experimental study using a centrifuge autoclave. J. Petrol. 39, 2095–2104.

Wallace, M.E., Green, D.H., 1988. An experimental determination of primary carbonatite magma composition. Nature 335, 343–346.

Watson, E.B., Harrison, T.M., 1983. Zircon saturation revisited-temperature and composition effects in a variety of crustal magma types. Earth. Planet. Sci. Lett. 64, 295–304.

Wingate, M.T.D., 2001. SHRIMP baddeleyite and zircon ages for an Umkondo dolerite sill, Nyanga Mountains, Eastern Zimbabwe. South Afr. J. Geol. 104, 13–22.

Wingate, M.T.D., Compston, W., 2000. Crystal orientation effects during ion microprobe U–Pb analysis of baddeleyite. Chem. Geol. 168, 75–97.

Wood, B.J., Blundy, J.D., 1997. A predictive model for rare earth element partitioning between clinopyroxene and anhydrous silicate melt. Contrib. Mineral. Petrol. 129, 166–181.

Yaxley, G.M., Green, D.H., 1996. Experimental reconstruction of sodic dolomitic carbonatite melts from metasomatised lithosphere. Contrib. Mineral. Petrol. 124, 359–369.

Yaxley, G.M., Crawford, A.J., Green, D.H., 1991. Evidence for carbonatite metasomatism in spinel peridotite xenoliths from western Victoria, Australia. Earth. Planet. Sci. Lett. 107, 305–317.

Yaxley, G.M., Green, D.H., Kamenetsky, V., 1998. Carbonatite metasomatism in the southeastern Australian lithosphere. J. Petrol. 39, 1917–1930.